Report No. NADC-91122-60

CORROSION BEHAVIOR OF SQUEEZE CAST ALUMINUM METAL MATRIX COMPOSITES

Vinod S. Agarwala, Ph.D. and Alan S. Fabiszewski
Air Vehicle and Crew Systems Technology Department (Code 6062)
NAVAL AIR DEVELOPMENT CENTER
Warminster, PA 18974-5000

DECEMBER 1991

FINAL REPORT
ONR R&T #45321

Approved for Public Release; Distribution is Unlimited.

Prepared for
OFFICE OF NAVAL RESEARCH (Code 1131)
800 North Quincy Street
Arlington, VA 22217-5000

NOTICES

REPORT NUMBERING SYSTEM — The numbering of technical project reports issued by the Naval Air Development Center is arranged for specific identification purposes. Each number consists of the Center acronym, the calendar year in which the number was assigned, the sequence number of the report within the specific calendar year, and the official 2-digit correspondence code of the Command Officer or the Functional Department responsible for the report. For example: Report No. NADC-88020-60 indicates the twentieth Center report for the year 1988 and prepared by the Air Vehicle and Crew Systems Technology Department. The numerical codes are as follows:

CODE	OFFICE OR DEPARTMENT
00	Commander, Naval Air Development Center
01	Technical Director, Naval Air Development Center
05	Computer Department
10	AntiSubmarine Warfare Systems Department
20	Tactical Air Systems Department
30	Warfare Systems Analysis Department
40	Communication Navigation Technology Department
50	Mission Avionics Technology Department
60	Air Vehicle & Crew Systems Technology Department
70	Systems & Software Technology Department
80	Engineering Support Group
90	Test & Evaluation Group

Reviewed By: Arthur Fletcher Date: 2/28/92
Branch Head

Reviewed By: [signature] Date: 3/2/92
Division Head

Reviewed By: [signature] Date: 3 Mar 92
Director/Deputy Director

REPORT DOCUMENTATION PAGE

Form Approved
OMB No 0704-0188

1. AGENCY USE ONLY *(Leave blank)*

2. REPORT DATE
December 1991

3. REPORT TYPE AND DATES COVERED
Final

4. TITLE AND SUBTITLE
Corrosion Behavior of Squeeze Cast Aluminum Metal Matrix Composites

5. FUNDING NUMBERS
ONR R&T #45321

6. AUTHOR(S)
Vinod S. Agarwala, Ph.D. and
Alan S. Fabiszewski

7. PERFORMING ORGANIZATION NAME(S) AND ADDRESS(ES)
Air Vehicle and Crew Systems Technology Department (6062)
NAVAL AIR DEVELOPMENT CENTER
Warminster, PA 18974-5000

8. PERFORMING ORGANIZATION REPORT NUMBER
NADC-91122-60

9. SPONSORING MONITORING AGENCY NAME(S) AND ADDRESS(ES)
OFFICE OF NAVAL RESEARCH
Code 1131
800 North Quincy Street
Arlington, VA   Dr. John A. Sedricks

10. SPONSORING/MONITORING AGENCY REPORT NUMBER

11. SUPPLEMENTARY NOTES

12a. DISTRIB[illegible]ON AVAILABILITY STATEMENT
Approved for Public Release; Distribution is Unlimited.

12b. DISTRIBUTION CODE

13. ABSTRACT *(Maximum 200 words)*

Corrosion behavior of metal matrix composites (MMC) vary greatly with the reinforcement material type, processing conditions and methods of fabrication into engineering parts. The corrosion susceptibilities for the MMC arise from the segregations of the reinforcement material during fluid flow (extrusion) and/or processing, and from the resulting compositional differences in the alloy, the matrix material. These differences sets-up galvanic cells and cause preferential corrosion. The metal matrix composites studied were Al 6061/Al_2O_3 and Al 356/SiC. In particular, the effects of near-net-shape processing called squeeze casting (solidification of liquid under pressure) was investigated. The results showed that regions which were clustered with SiC or Al_2O_3 were microstructurally sensitive to preferential corrosion. Electrochemical potentiodynamic polarization and controlled potential corrosion behavior measurements were made and related to microstructural segregation through metallographic optical microscopic analysis.

14. SUBJECT TERMS
Squeeze Cast (near net shape processing), Aluminum oxide, Silicon Carbide, 6061 & 356 aluminum, Preferential attack, Electrochemical testing (potentiodynamic, potentiostatic)

15. NUMBER OF PAGES
24

16. PRICE CODE

17. SECURITY CLASSIFICATION OF REPORT	18. SECURITY CLASSIFICATION OF THIS PAGE	19. SECURITY CLASSIFICATION OF ABSTRACT	20. LIMITATION OF ABSTRACT
Unclassified	Unclassified	Unclassified	Unlimited

GENERAL INSTRUCTIONS FOR COMPLETING SF 298

The Report Documentation Page (RDP) is used in announcing and cataloging reports. It is important that this information be consistent with the rest of the report, particularly the cover and title page. Instructions for filling in each block of the form follow It is important to ***stay within the lines*** to meet ***optical scanning requirements***.

Block 1. Agency Use Only *(Leave blank)*.

Block 2. Report Date. Full publication date including day, month, and year, if available (e.g. 1 Jan 88). Must cite at least the year.

Block 3. Type of Report and Dates Covered. State whether report is interim, final, etc. If applicable, enter inclusive report dates (e.g. 10 Jun 87 - 30 Jun 88).

Block 4. Title and Subtitle. A title is taken from the part of the report that provides the most meaningful and complete information. When a report is prepared in more than one volume, repeat the primary title, add volume number, and include subtitle for the specific volume. On classified documents enter the title classification in parentheses

Block 5. Funding Numbers To include contract and grant numbers; may include program element number(s), project number(s), task number(s), and work unit number(s) Use the following labels:

C -	Contract	**PR** -	Project
G -	Grant	**TA** -	Task
PE -	Program Element	**WU** -	Work Unit Accession No

Block 6. Author(s) Name(s) of person(s) responsible for writing the report, performing the research, or credited with the content of the report If editor or compiler, this should follow the name(s).

Block 7. Performing Organization Name(s) and Address(es) Self-explanatory

Block 8. Performing Organization Report Number Enter the unique alphanumeric report number(s) assigned by the organization performing the report

Block 9. Sponsoring/Monitoring Agency Name(s) and Address(es) Self-explanatory

Block 10. Sponsoring/Monitoring Agency Report Number *(If known)*

Block 11. Supplementary Notes Enter information not included elsewhere such as: Prepared in cooperation with ; Trans. of , To be published in When a report is revised, include a statement whether the new report supersedes or supplements the older report

Block 12a. Distribution/Availability Statement. Denotes public availability or limitations. Cite any availability to the public Enter additional limitations or special markings in all capitals (e.g. NOFORN, REL, ITAR).

DOD - See DoDD 5230.24, "Distribution Statements on Technical Documents."
DOE - See authorities.
NASA - See Handbook NHB 2200.2
NTIS - Leave blank.

Block 12b. Distribution Code.

DOD - Leave blank.
DOE - Enter DOE distribution categories from the Standard Distribution for Unclassified Scientific and Technical Reports.
NASA - Leave blank
NTIS - Leave blank

Block 13. Abstract Include a brief *(Maximum 200 words)* factual summary of the most significant information contained in the report.

Block 14. Subject Terms Keywords or phrases identifying major subjects in the report.

Block 15. Number of Pages Enter the total number of pages

Block 16. Price Code Enter appropriate price code *(NTIS only)*

Blocks 17. - 19. Security Classifications Self-explanatory Enter U S Security Classification in accordance with U S Security Regulations (i e , UNCLASSIFIED) If form contains classified information, stamp classification on the top and bottom of the page

Block 20. Limitation of Abstract This block must be completed to assign a limitation to the abstract. Enter either UL (unlimited) or SAR (same as report). An entry in this block is necessary if the abstract is to be limited If blank, the abstract is assumed to be unlimited

TABLE OF CONTENTS

LIST OF TABLES

Table | Page

LIST OF FIGURES

Introduction

Metal Matrix Composites (MMC) are highly heterogeneous in nature, and exhibit a high degree of anisotropy in their properties. This is further complicated by the heat treatments, and various fabrication and processing techniques employed to manufacture finished parts. Generally, it is the matrix material which is affected by processing and becomes susceptible to corrosion; compositional differences play a major role in setting up the galvanic corrosion cells. Past studies have focused on such fabrication and processing variables as variation in matrix composition, particulate vs. whisker reinforcement, extrusion ratio, and the heat treatments (1-4).

In earlier studies MMC's were reported to corrode preferentially at the surface layers and in the interfacial regions of the reinforcement and matrix (1,3,4). Thermal conductance mismatch between the matrix material (highly conductive aluminum alloy) and the ceramic reinforcement (non-conducting oxides, carbides etc.) create heat effected zones in the interfacial region of the particulate and the matrix, thus contributing more toward the heterogeneity in the microstructure. Thermal gradients cause compositional changes in the alloy locally with the segregation of elements in the matrix constituents, form voids and also possibly cause reduction of the reinforcement material such as alumina to aluminum (1,3). Generally, these segregations were significant enough to set-up galvanic cells and cause preferential corrosion in these regions. Reinforcement type, particulate or whisker, can have an effect on preferential corrosion (3). During processing whiskers have a great tendency not only to be flawed but to become misaligned and cluster together in some areas whereas leaving other areas devoid of reinforcement material (1,5-7). Enhanced preferential corrosion was observed in those clustered areas. Even in the materials where particulate distribution was much more uniform, there were still some clustered areas which exhibited enhanced corrosion attack (2,3). The increasing extrusion ratio can help to elevate this problem with the particulate reinforcement and produce a more homogeneous MMC. However, the whiskers under great extrusion pressures could get damaged, thus a composite may loose its mechanical advantage (4,5).

Work-hardening (plastic deformation) or recrystallization produced during the extrusion and machining (fabrication) are conventionally removed by heat treatments In case of MCC, conventional solution heat treatments were found to be inadequate to relieve prior cold working; rather, it made the composite more susceptible to corrosion (1). The lack of thermal conductivity across the reinforcement material was the reason considered. A higher temperature post solution heat-treatment for longer times was required not only to reduce segregation and preferential attack but also to enhance corrosion resistance of the composite, in general. It was believed that the MMC may have become more homogeneous and free of the residual stresses with this treatment (1).

The manufacture of finished products from MMC has been greatly impacted by their susceptibility to microstructural corrosion due to the effects of processing and fabrication. Any machining of the part after the heat treatment shall be a cause for great concern. A number of MMCs, in particular, 6061-SiCw and 2124-SiCw composite materials have been planned for use in military aircraft tail wing structures. The effects of processing variables such as extrusion, continuous and squeeze casting, and heat treatment may have tremendous consequences on the properties of MMCs (8-9). An optical metallographic examination of microstructural segregation and the analysis of corrosion behavior through controlled potential electrochemical polarization measurements would be highly significant in determining the areas of preferential segregation and corrosion susceptibility.

In this study, the effects of near-net-shape processing, called squeeze casting (solidification of liquid under pressure) on the corrosion susceptibility of MMCs containing SiC and Al_2O_3 as reinforcement particulates in two Al alloy matrices has been investigated. Extrusions and cast billets of aluminum alloy specimens were used for comparison. The electrochemical polarization, corrosion (mass-loss) and metallographic optical microscopic techniques were employed in the investigations.

Experimental Procedure

Material : The materials used for this study were 356 Al+20% SiC squeeze cast, 356 Al+15% SiC cast billet, 6061 Al+15% Al_2O_3 squeeze cast, and 6061+ Al_2O_3 extrusion. A schematic chart depicting the production sequences of the composites were as shown in Figures 1 and 2. The nominal compositions of the Al 356 and Al 6061 alloys are as follows:

Al 6061 alloy: Mn, 0.15; Fe, 0.7; Si, 0.8; Cr, 0.3; Ti, 0.15 Mg, 1.0; Cu, 0.4; Zn 0.25 and Al, balance.

Al 356 alloy : Mn, 0.05; Fe, 0.2; Si, 7.0; Ti, 0.2; Mg, 0.4; Cu, 0.1; Zn, 0.05 and Al, balance.

Corrosion Studies : The general corrosion behavior of the MMC's were determined by performing mass-loss total immersion tests in 3.5% NaCl solutions of pH 2 and 6. Coupon specimens from the short transverse-longitudinal (S-L) face were used. The specimens were exposed for 7 days after which time they were removed from the solutions and cleaned in 50v/o nitric acid then dried before final weighing. The test was performed according to ASTM Standard Method G 31-72 (10).

Electrochemical Studies : Measurements of open circuit (corrosion) potentials, potentiodynamic polarization (E vs. log i) and controlled potential (i vs time) were

Ceramic Reinforcement

↓

Deagglomeration **Metal Powder**

↓

Mixing and Degassing

↓

Billet Cosolidation

↓

Primary Processing
(Rolling, Extrusion, Forging)

↓

Secondary Processing
(Forming, Joining, Machining)

Figure 1. Schematic of PM-MMC fabrication (ref 8.)

Die/preform heating

↓

Molten- metal pouring

↓

High pressure infiltration

↓

Removal of composites

Figure 2. Schematic of the squeeze-casting process (ref 9.)

conducted on the MMC's. Corrosion current densities, polarization resistances and the anodic and cathodic Tafel slopes were determined from these measurements. The test solutions used were 3.5% NaCl, pH 2 and 6. A saturated calomel reference electrode and a platinum counter electrode were employed.

Specimens were cold mounted in epoxy with their short transverse-longitudinal (S-L) face exposed. The surface was prepared by using an automatic grinding/polishing unit which uses diamond polishing media. This technique proved to give the most reproducible surface finishes. It also minimized particle tear-out which is always accompanied with materials containing hard facing substances (reinforcements).

The potentiodynamic polarization measurements were run in the potential range of -1.4 V to -0.4 V with a scan rate of 0.166 mV/second. The potential was scanned from the cathodic to the anodic region. In most cases the scans were started as soon as the specimens were put into the solution, however, in few cases, a delay prior to the scan was used to determine the open circuit (corrosion) potential.

Controlled Potential (i vs t) measurements were conducted at settings of -0.50 V for 30min; -0.70 V for 60min and -0.90 V for 120min. The metallographically polished specimens of each MMC's were run at the above settings so the results could be compared. The potential was controlled as soon as the specimen was immersed in the solution. All electrochemical measurements were performed with a PAR Model 351-2 Corrosion Measuring System in accordance with ASTM Standard Methods G 3-74 and G 5-82 (11,12).

Optical Microscopic Analysis : The metallographically polished specimens were examined before and after total immersion tests under controlled potential polarization condition, and at three potentials as described earlier. Specimens were also examined after being etched with Kellers Reagent. An optical metallograph was used to observe SiC and Al_2O_3 distribution, and the preferential attack, if any.

Results and Discussion

The data for the mass-loss (total immersion) tests for each MMC's have been summarized in Table I. The corrosion rates reported are in mdd (mils decimeter squared day). The 356+15% SiC billet showed the lowest rate in the pH 6 solution followed by the 356+20% SiC squeeze cast, 6061+15% Al_2O_3 extrusion and 6061+15% Al_2O_3 squeeze cast. In pH 2 solution, the order changed with the 356+20% SiC squeeze cast having the lowest rate, then 356+15% SiC billet. The 6061+15% Al_2O_3, both the extrusion and squeeze cast, were almost one and a half times greater than for Al 356+SiC in the squeeze cast condition. A significant thing to note was that there was almost no difference between the corrosion rates of the extrusion and squeeze cast specimens for

the 6061+15% Al_2O_3 MMCs. It must be understood that the mass-loss tests reflect only average corrosion rates over the entire surface area. Under preferential attack, corrosion rates can very high in certain areas and may vary from region to region along the whole of the MMC material.

TABLE I
TOTAL IMMERSION WEIGHT LOSS CORROSION RATES

Materials	Corrosion Rates (mdd) pH 6	pH 2
6061 + 15% Al_2O_3 extrusion	66.86	423.29
6061 + 15% Al_2O_3 sq cast	67.46	482.35
356 + 15% SiC cast billet	35.09	284.26
356 + 20% SiC sq cast	48.31	260.12

The potentiodynamic polarization behavior for the MMC's in pH 2 and 6 are given in Figures 3 and 4 respectively. The E vs log i curves showed no significant differences between the two processing techniques. Only subtle differences existed which are summarized in Tables 2 and 3 as electrochemical parameters. In pH 2 solution, the 356+20% SiC squeeze cast had the lowest corrosion current density. It was just slightly lower than the 356+15% SiC billet but almost half as great as both the extruded and squeeze cast 6061+15% Al_2O_3. The pH 6 solution produced slightly different results. The 356+15% SiC billet had the lowest current density followed by 356+20% SiC squeeze cast, 6061+15% Al_2O_3 extrusion, and 6061+15% Al_2O_3 squeeze cast respectively. Corrosion current density results in both pH solutions corresponded well with the results from the mass-loss tests.

TABLE II
TYPICAL ELECTROCHEMICAL PARAMETERS OF MATERIALS IN 3.5% NaCl SOLUTIONS AT pH 2

Electrochemical Parameters	MMC's 6061+15% Sq	6061+15% Ext	356+20% Sq	356+15% Billet
E_{OC}, mV	-.742	-.756	-.760	-.766
R_p, $\Omega * cm^2$	5.00e3	4.85e3	9.11e3	3.75e3
E(I=0), mV	-.828	-.833	-.780	-.792
βc, mV/dec	320	417	262	261
βa, mV/dec	67	89	56	46
I_{CORR}, A/cm^2	14.20e-6	13.10e-6	6.69e-6	7.22e-6

TABLE III
TYPICAL ELECTROCHEMICAL PARAMETERS OF MATERIALS IN 3.5% NaCl SOLUTIONS AT pH 6

Electrochemical Parameters	MMC's 6061+15% Sq	6061+15% Ext	356+20% Sq	356+15% Billet
E_{OC}, mV	-.723	-.714	-.768	-.752
R_p, $\Omega * cm^2$	1.06e3	2.83e3	2.18e3	5.98e3
E(I=0), mV	-.695	-.671	-.736	-.717
βc, mV/dec	477	-3383	7656	708
βa, mV/dec	49	46	51	41
I_{CORR}, A/cm^2	6.04e-6	4.48e-6	3.96e-6	2.44e-6

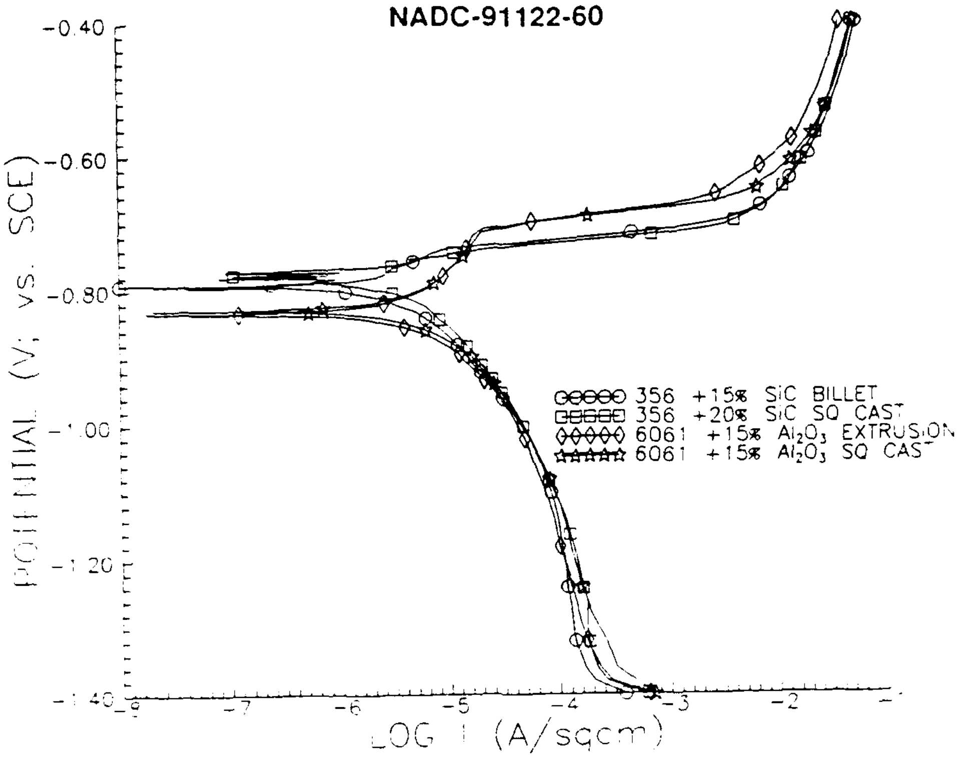

Figure 3. Potentiodynamic polarization behavior of the MMCs in 3.5% NaCl pH 2 solution.

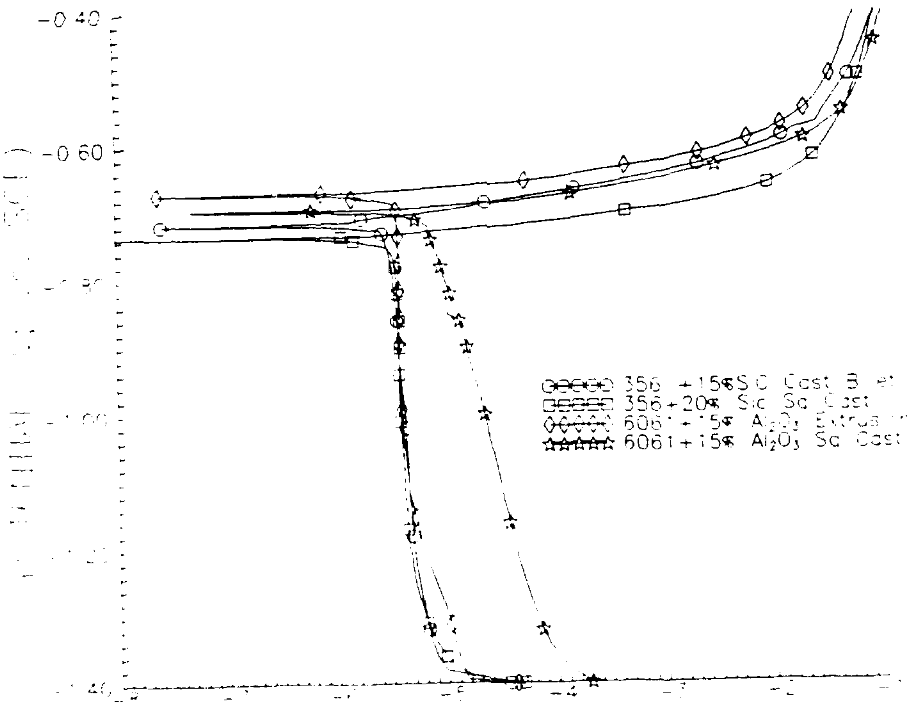

Figure 4. Potentidynamic polarization behavior of the MMCs in 3.5% NaCl pH 6 solution.

Constant potential (potentiostatic) tests were used to study preferential corrosion behavior of the MMCs. Their current density transients can be observed at the various settings in Figures 5, 8, and 11. By using these plots along with optical microscopic evaluation, the selective microstructural attack of the composites was studied. The three potentials chosen were picked from the potentiodynamic scans in pH 2 solution. These corresponded with the corrosion potential (-0.70 V) and the potentials 200 mV in the cathodic and anodic regions, i.e., -0.50 V and -0.90 V, respectively. The first set of tests were run at the anodic potential or under highly severe condition, at -0.50 V for 30 minutes. At this potential except for highly noble constituents, everything should be susceptible to corrosion. As shown in Figure 5, 356+20% SiC squeeze cast showed a steady-state dissolution current density of approx. 60 mA/cm^2; this was almost twice than that for the other three samples. On examining the micrographs in Figures 6 (at 100X) and 7 (at 1000X), it was found that the 356+20% SiC squeeze cast was preferentially attacked in the particulate clustered regions (Fig. 6A). At a higher magnification (Fig. 7A) the micrograph showed loss of

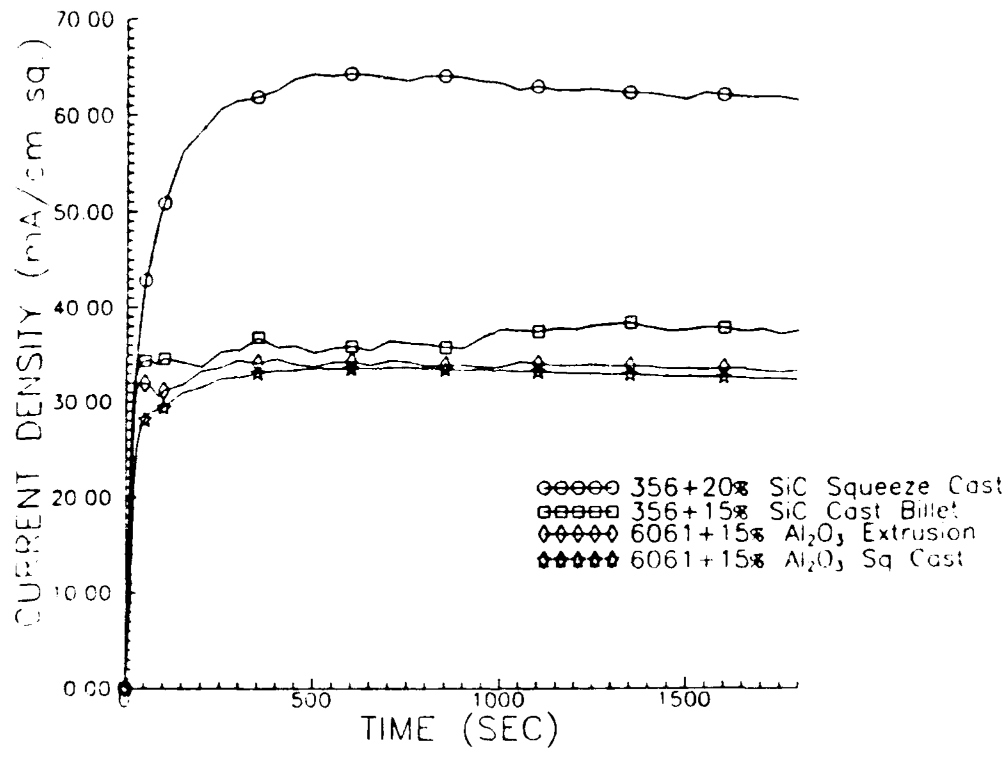

Figure 5. Potentiostatic behavior of the MMCs at -0.5volts for 30min in 3.5% NaCl pH 2 solution.

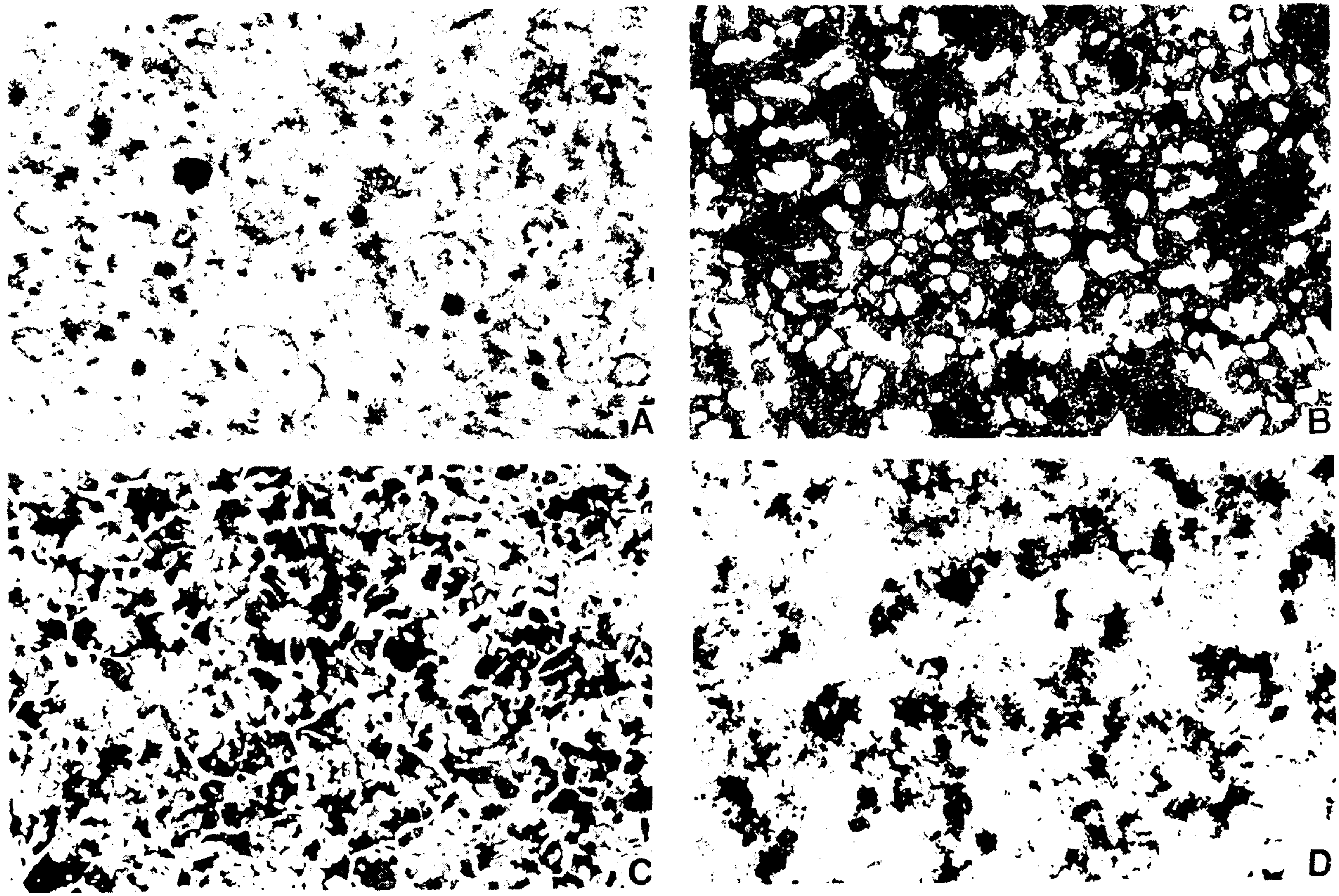

Figure 6. Optical micrographs of MMCs after controlled potential exposure at -0.5volts for 30minutes 100x. A) 356+20% SiC sq cast; B) 356+15% SiC billet; C) 6061+15% Al_2O_3 extrusion; D) 6061+15% Al_2O_3 sq cast.

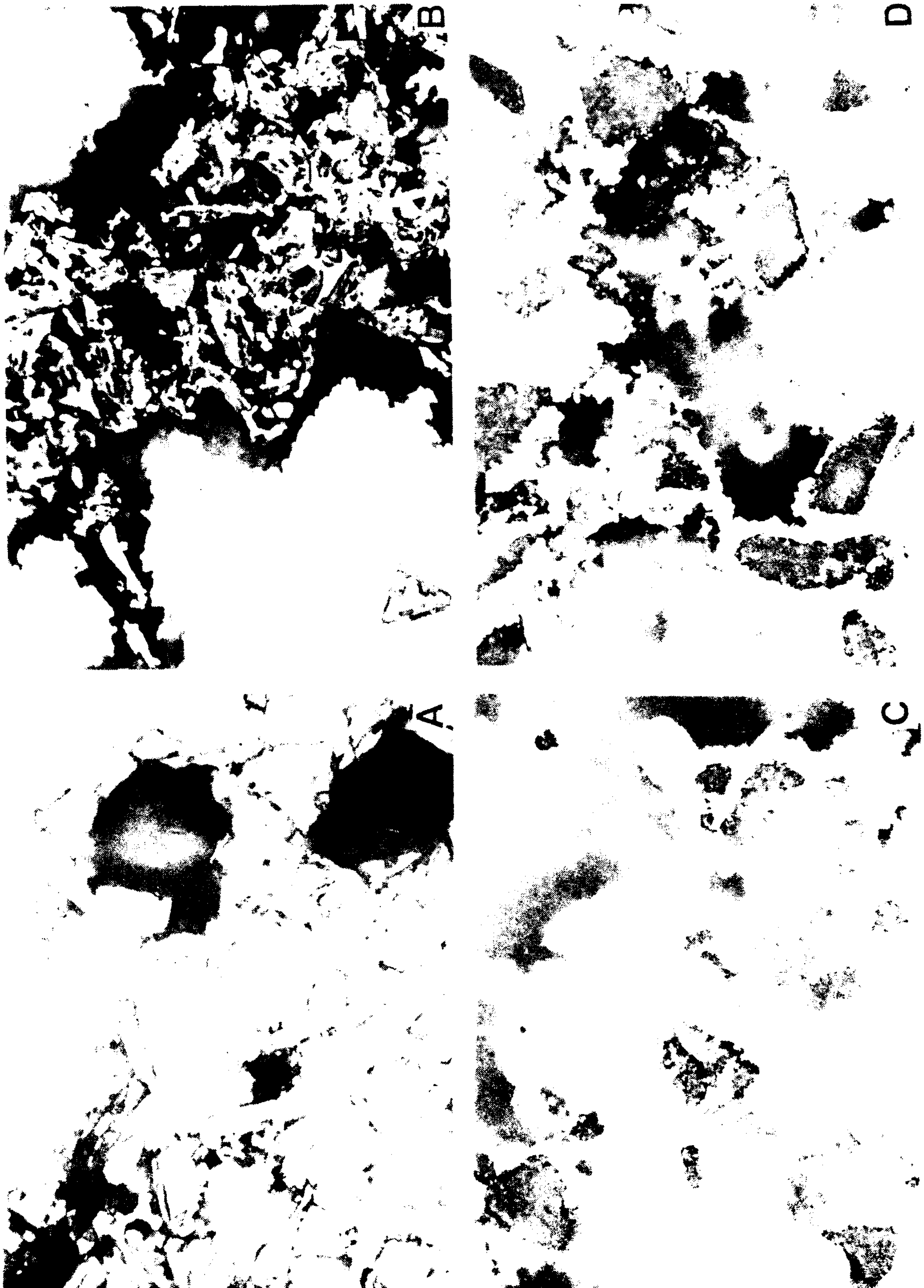

Figure 7. Optical micrographs of MMCs after controlled potential exposure at -0.5volts for 30minutes 1000x. A) 356+20% SiC sq cast; B) 356+15% SiC billet; C) 6061+15% Al_2O_3 extrusion; D) 6061+15% Al_2O_3 sq cast.

particulates (SiC) due to the dissolution of the matrix in the interfacial region. The 356+15% SiC billet (Fig. 6B) also appeared severely attacked in the clustered regions; however, when examined more closely at a higher magnification (Fig.7B), there was severe corrosion of the matrix in the vicinity of SiC particulates. The matrix area which was devoid of particulate appeared free of selective attack. The 6061+15% Al_2O_3 squeeze cast and extrusion showed nearly the same current density versus time curve at -0.50 V for 30 minutes (Fig.5). The micrographs of the 6061+15% Al_2O_3 squeeze cast showed (Fig. 6D) that it had a much more uniform distribution of Al_2O_3 particulates than the one with extrusion (Fig. 6C). Both processes (squeeze cast and extrusion) showed heavy preferential corrosion and pitting, in or near the particulate clusters (Figs. 7C & 7D). There were some areas, away from the particulate, where matrix was also attacked. This along with the severe attack of the matrix in the immediate vicinity of particulates (interfacial regions) caused heavy loss of the reinforcement.

The next set of potential control tests were run at -0.70 V for 60 minutes. Because this potential was near the corrosion potential, it could be possible to determine how processing conditions could alter the general corrosion behavior of the MMCs. If as a

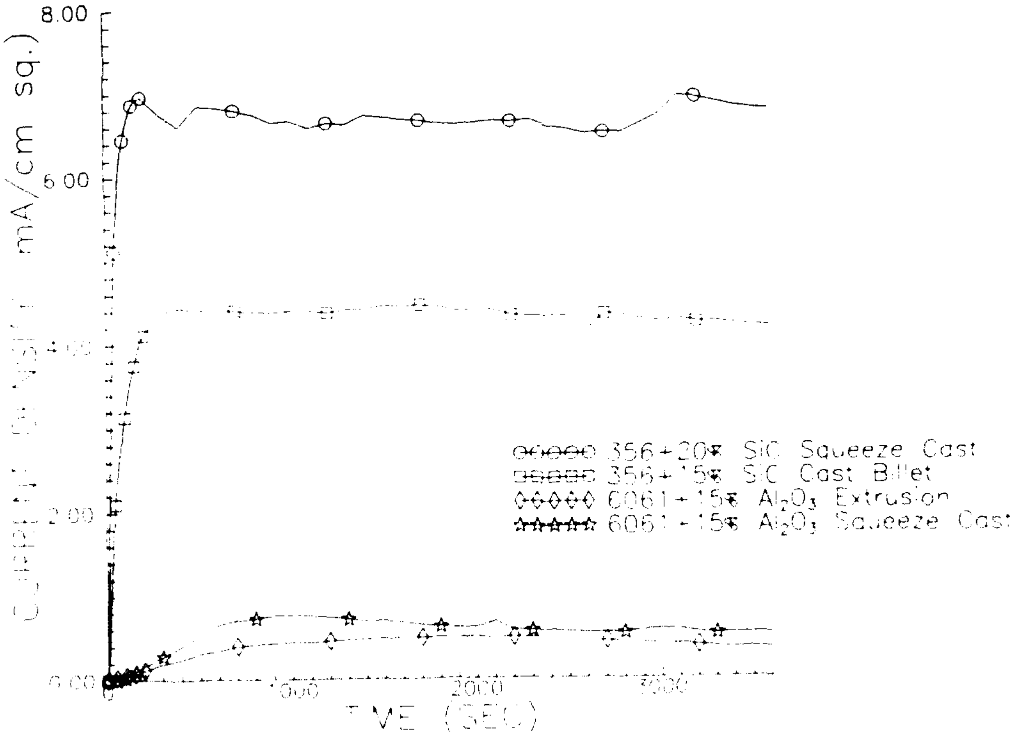

Figure 8. Potentiostatic behavior of the MMCs at -0.7volts for 60min in 3.5% NaCl pH 6 solution.

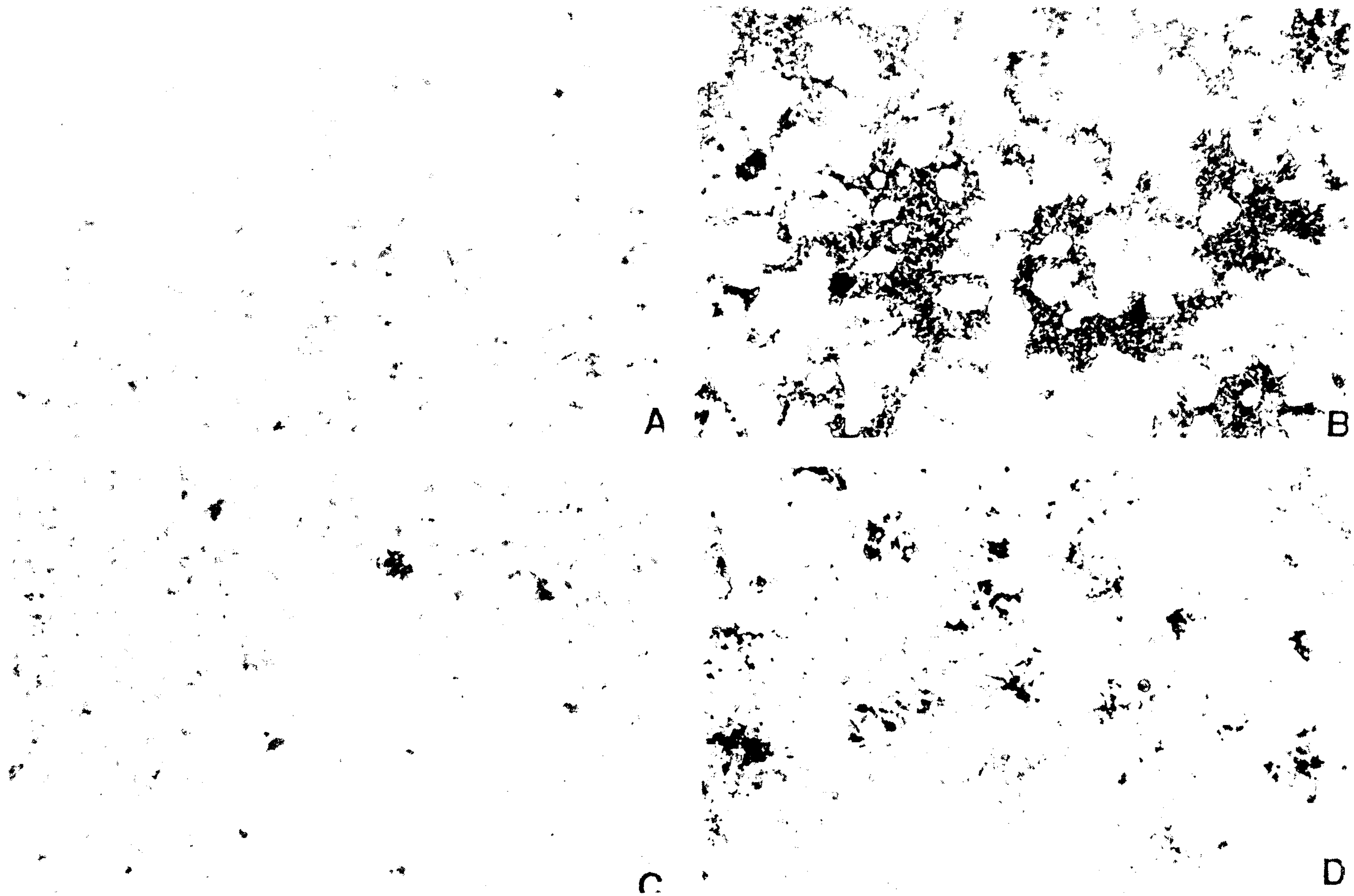

Figure 9. Optical micrographs of MMCs after controlled potential exposure at -0.7volts for 60minutes 100x. A) 356+20% SiC sq cast; B) 356+15% SiC billet; C) 6061+15% Al_2O_3 extrusion; D) 6061+15% Al_2O_3 sq cast.

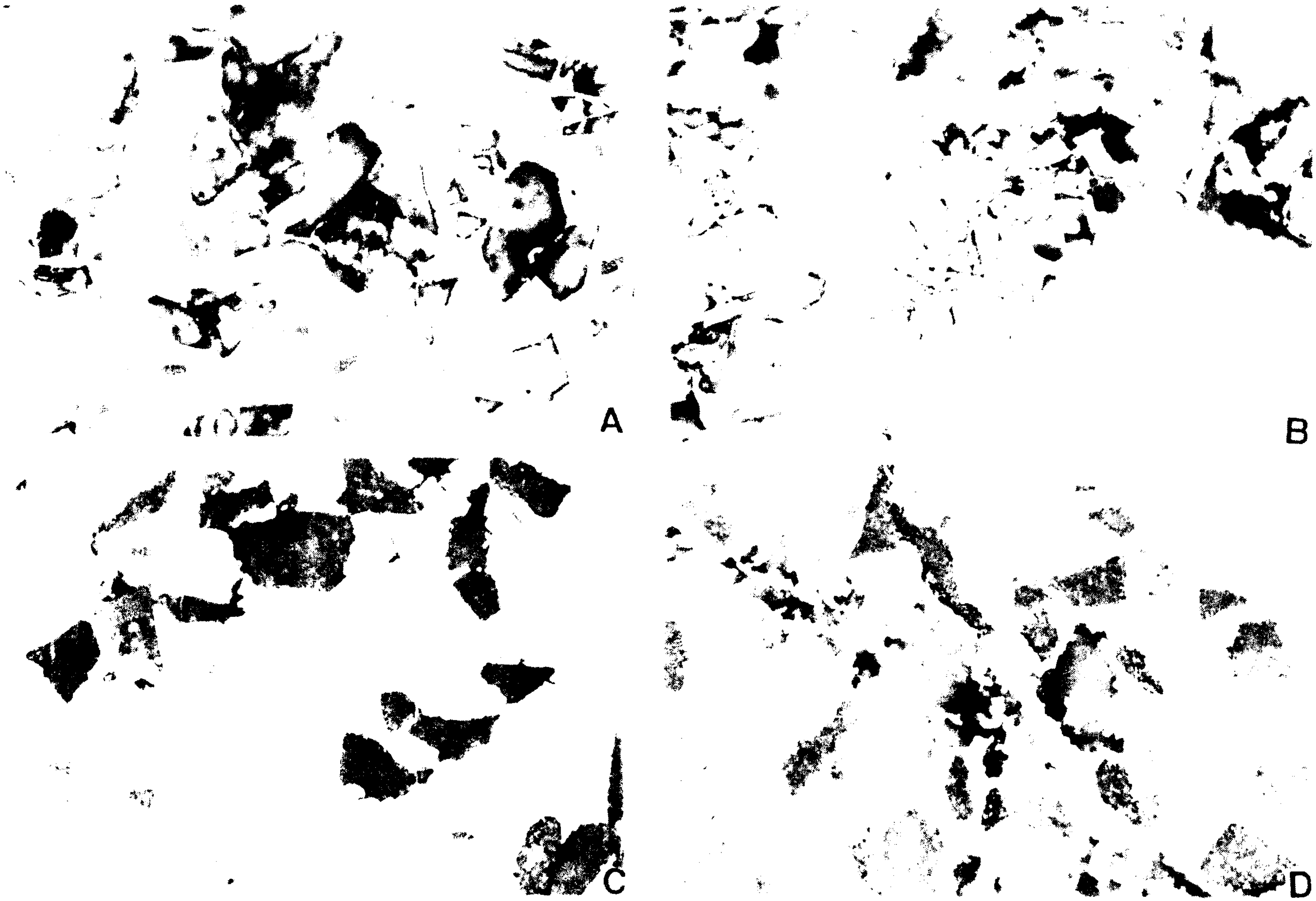

Figure 10. Optical micrographs of MMCs after controlled potential exposure at -0.7volts for 60minutes 1000x. A) 356+20% SiC sq cast; B) 356+15% SiC billet; C) 6061+15% Al_2O_3 extrusion; D) 6061+15% Al_2O_3 sq cast.

result of processing some dealloying (elemental redistribution or segregation) of the matrix material occurred, the regions devoid of noble constituents (elements) would become anodic to the bulk alloy composition and corrode preferentially. A plot of current density versus time and the micrographs for the exposed specimens at this potential are shown in Figure 8, and Figures 9 and 10, respectively. The 356+20% SiC squeeze cast sample again showed the highest corrosion current density, ~7 UA/cm^2, which was about 1.5 times greater than the 356+15% SiC billet and almost 7 times as great as both the 6061+15% Al_2O_3 squeeze cast and extrusion (Fig.8) showed that at the early stages of controlled potential exposure, severe selective attack occurred in the regions where the particulates clustered. In fact, it was very severe around the particulate itself, as shown in Fig. 10A, at 1000X magnification. The 356+15% SiC billet also experienced similar initial attack within the particulate clustered region (cf. Figure 9B & 9B). Some particulates have been shown to fall-out in both specimens within the clustered areas (cf. Figs. 9B & 9B). Though, very little preferential corrosion occurred in the immediate vicinity of the particulate, and the matrix was virtually unaffected. It suggested that matrix in the clustered region had become very susceptible to corrosion either because of some noble potential behavior of the SiC particulates or compositionally that corroded area was devoid of some noble constituents. The 6061+15% Al_2O_3 specimens, both the extrusion and squeeze cast, showed very little corrosion attack at -0.70 V (Figs. 9C & 9D). The selective attack however was not seen to be limited to the clustered areas or at the interface region of the matrix and particulates (Figs. *10C & 10D). Selective corrosion* occurred in the region within the matrix which were devoid of any reinforcement material. The squeeze cast showed less of this type of corrosive attack (Fig. 10D). At this point, signs of grain boundary corrosion also began to appear.

The plots of current transients at -.90 V for 120 minutes showed a negative current or cathodic polarization behavior for all MMCs (Fig 11). The Al 6061/Al_2O_3 composites showed highly cathodic behavior which increased with time. Most probably, the currents were involved in the process none other than evolution of hydrogen; as the surface got more & more cleaner due to reduction of the surface oxide or the reinforcement, the rate of hydrogen reduction reaction increased. Since there was almost no anodic dissolution involved, the optical micrographs of the specimens showed no visible attack at all (cf. Figs. 12 & 13, plates C & D). Even Al 356/SiC composites were unaffected at this potential. There may have been some interfacial regions near the particulates where some etching could be observed (Figs. 12 & 13, plates A & B).

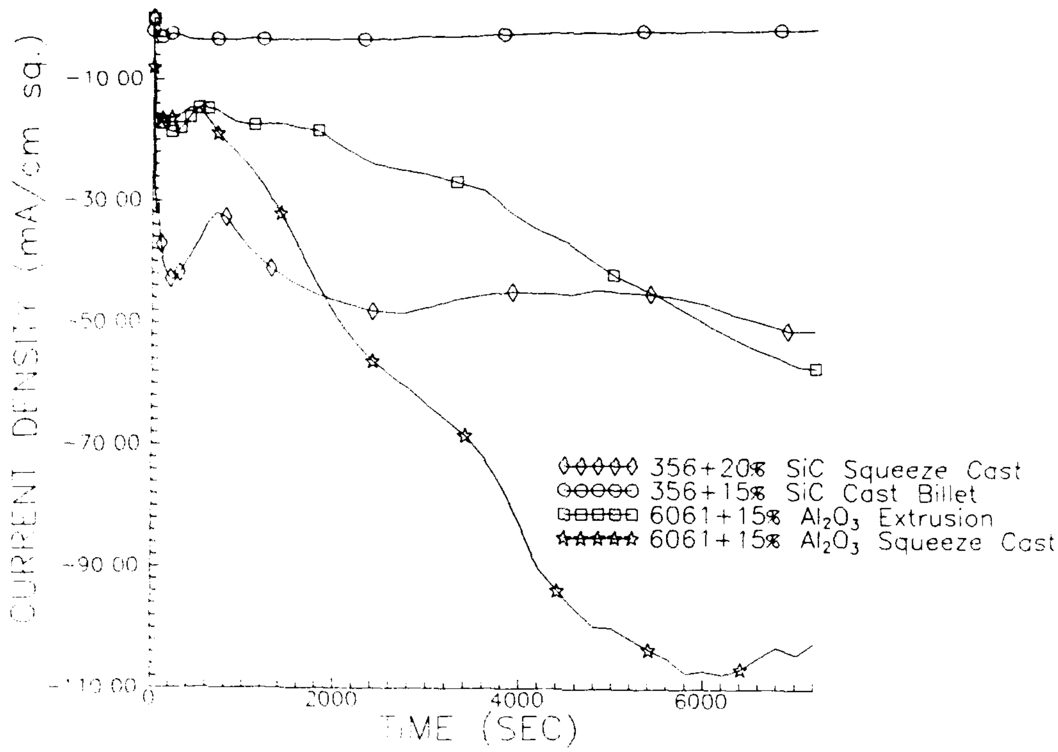

Figure 11. Potentiostatic behavior of the MMCs at -0.9volts for 120min in 3.5% NaCl pH 2 solution.

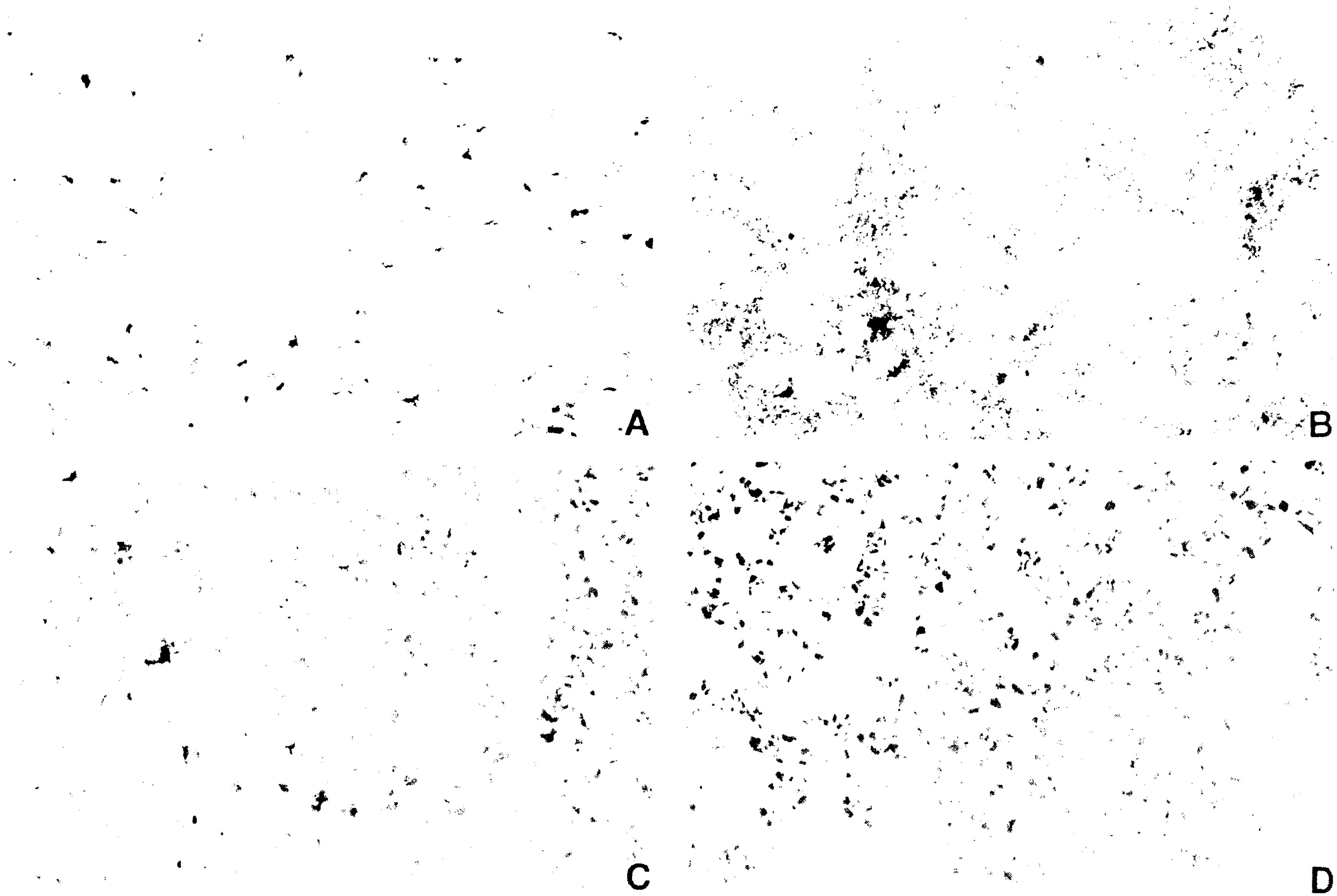

Figure 12. Optical micrographs of MMCs after controlled potential exposure at -0.9volts for 120minutes 100x. A) 356+20% SiC sq cast; B) 356+15% SiC billet; C) 6061+15% Al_2O_3 extrusion; D) 6061+15% Al_2O_3 sq cast.

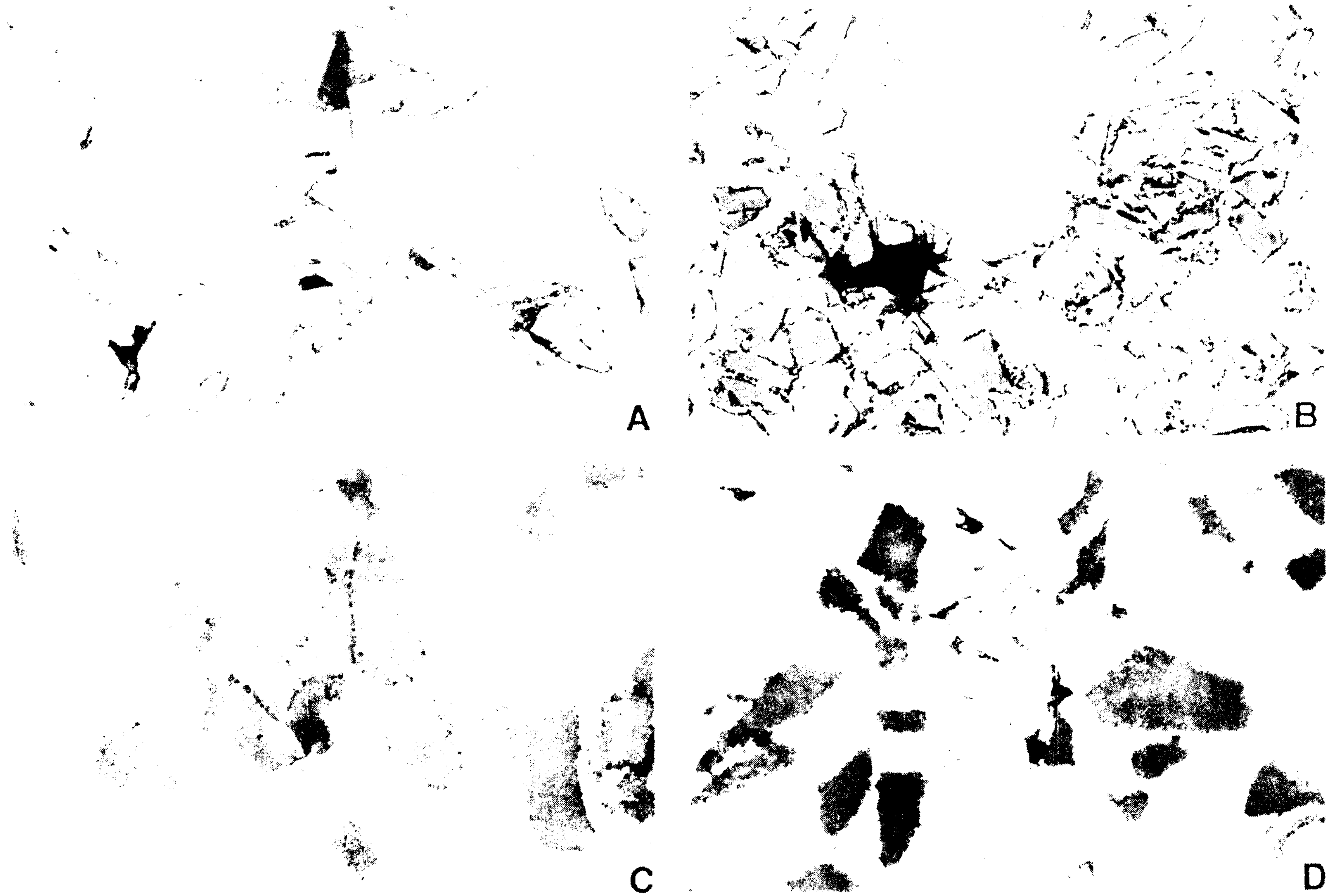

Figure 13. Optical micrographs of MMCs after controlled potential exposure at -0.9volts for 120minutes 1000x. A) 356+20% SiC sq cast; B) 356+15% SiC billet; C) 6061+15% Al_2O_3 extrusion; D) 6061+15% Al_2O_3 sq cast.

By careful examination of the microstructures it was possible to differentiate the effects the processing had on the orientation of the microstructure(Figure 14). It was found that the ceramic reinforcement clustered in the interdendritic spaces during casting of Al 356+15% SiC billet. This is known to occur during slow cooling at which time the moving liquid-solid interface forces the ceramic reinforcement into the interdendritic spaces (13). The 356+20% SiC squeeze cast had a more homogeneous dispersion of the particulate matter; due in part to the processing and the increase in overall volume fraction of the particulates. There was little difference in particulate distribution between the 6061+15% Al_2O_3 squeeze cast and extrusion. The squeeze cast material showed less clustering than the extrusion. The micrographs also showed voids on the composite. These voids could be either from processing or could have occurred during polishing (tear-out). Although, even the most careful surface preparation techniques could not avoids tearing, it was believed that voids were inherent with the composite processing.

Etching the specimens with Kellers Reagent revealed the secondary phases within the microstructures of MMCs. Mostly, secondary phases can act as pit initiation sites (14) . In heterogeneous systems, such as MMCs, the processing conditions form intermetallic phases or inclusions which become the sites for pit initiation (14). On examining the micrographs of the etched specimens before the controlled potential tests, it was revealed that in the case of Al 356/SiC composites (shown in Figs. 15 & 16, plates A & B) secondary phases appear d mainly within the particulate clustered regions and only in small amounts around the individual reinforcement itself. This corresponded well with the preferential attack noted in the micrographs taken after the controlled potential tests at -0.50 V and -0.70 V.

The etched Al 6061/Al_2O_3 composites showed large secondary phases primarily around the particulate with few large areas in the matrix region which were devoid of the reinforcement (Figs. 15 & 16, plated C & D). This explains the selective attack in the region for Al 6061/Al_2O_3 as found in the micrographs after the controlled potential tests. This also corresponded well with the conclusion that during processing and heat treatment segregation of the elemental constituents could occur.

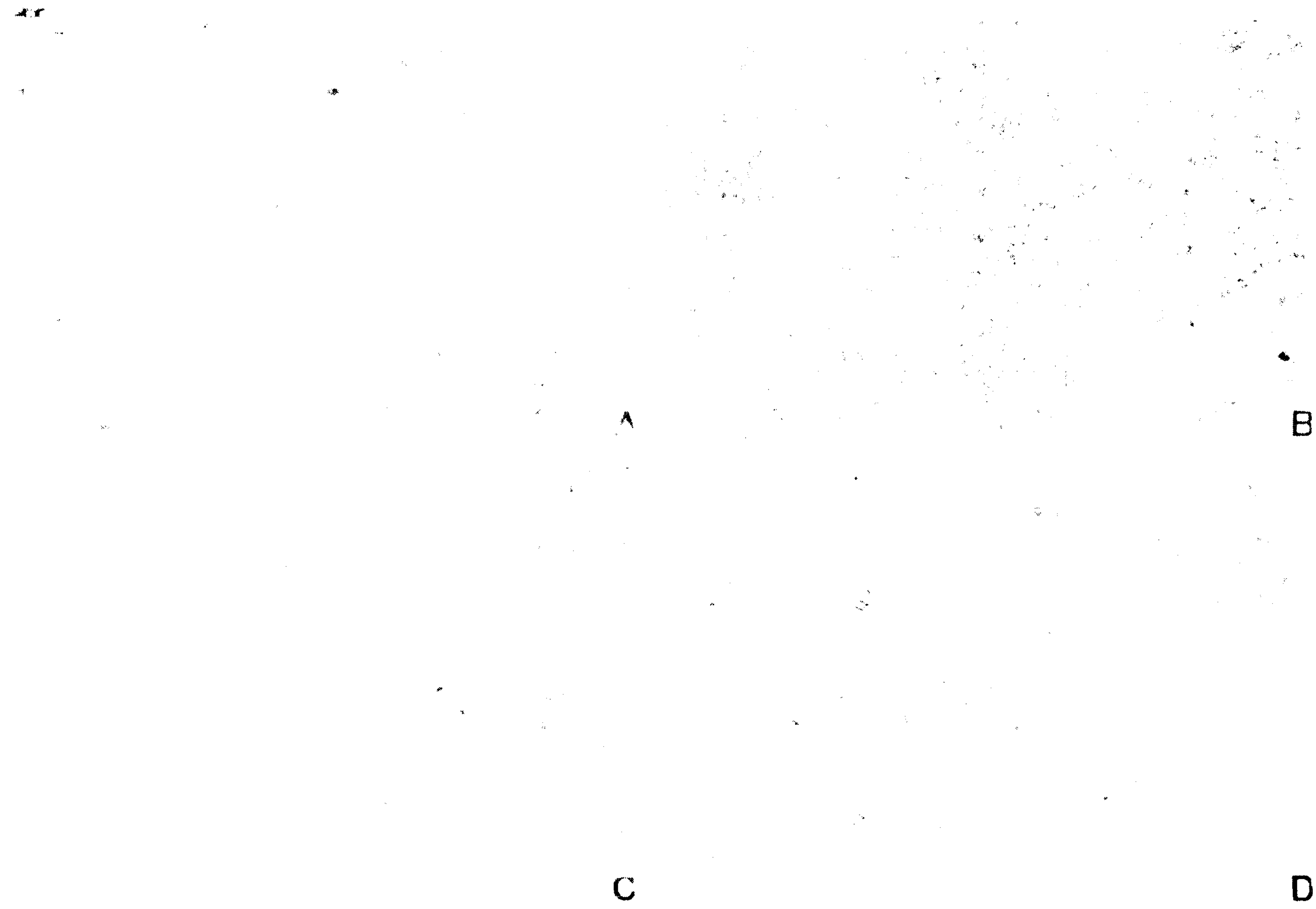

Figure 14. Optical micrographs of MMCs as receiced 100x. A)356+20% SiC sq cast B) 356+15% SiC billet; C) 6061+15% Al_2O_3 extrusion; D) 6061+15% Al_2O_3 sq cast.

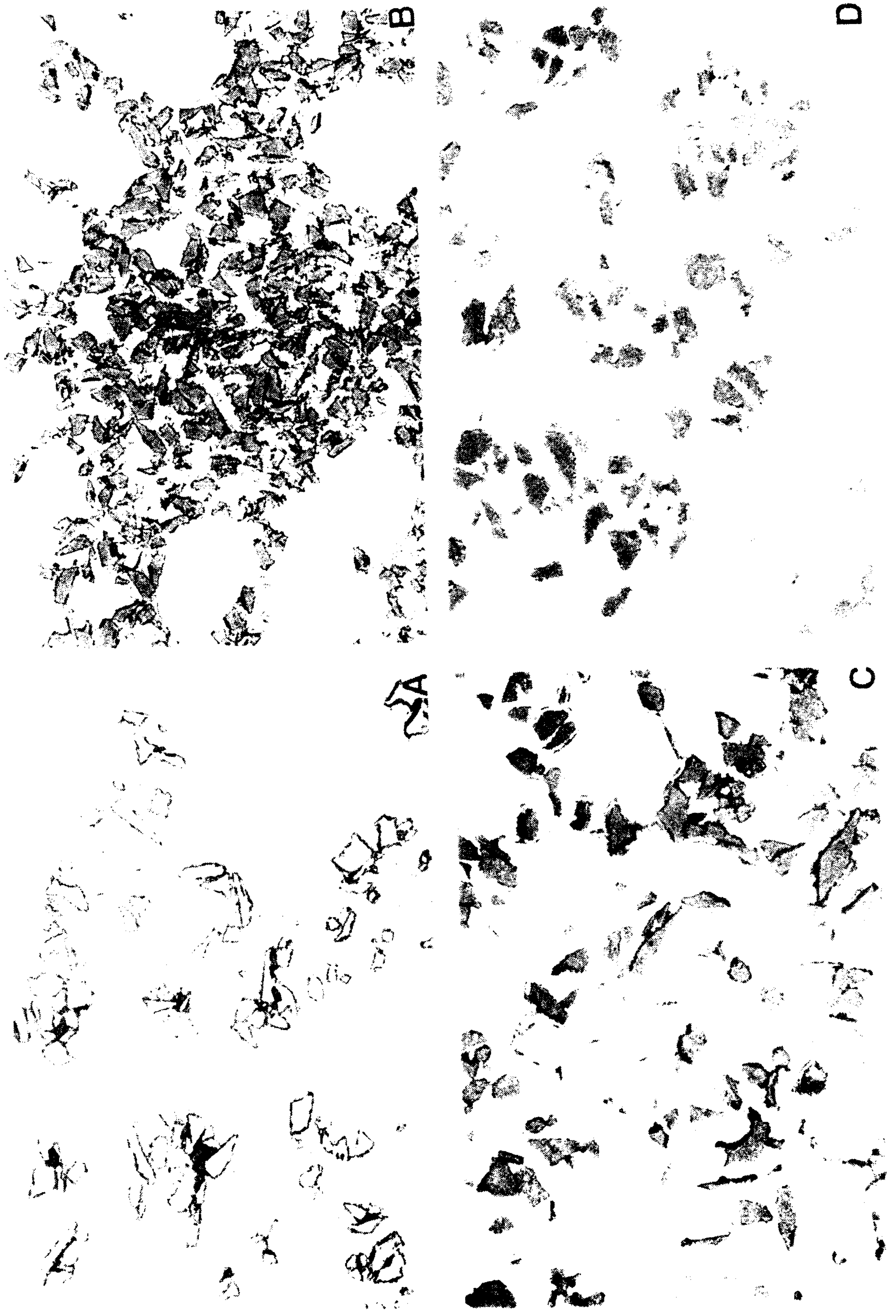

Figure 15.. Optical micrographs of MMCs etched with Kellers reagent at 400x A) 356+20% SiC sq cast; B) 356+15% SiC billet; C) 6061+15% Al_2O_3 extrusion; D) 6061+15% Al_2O_3 sq cast.

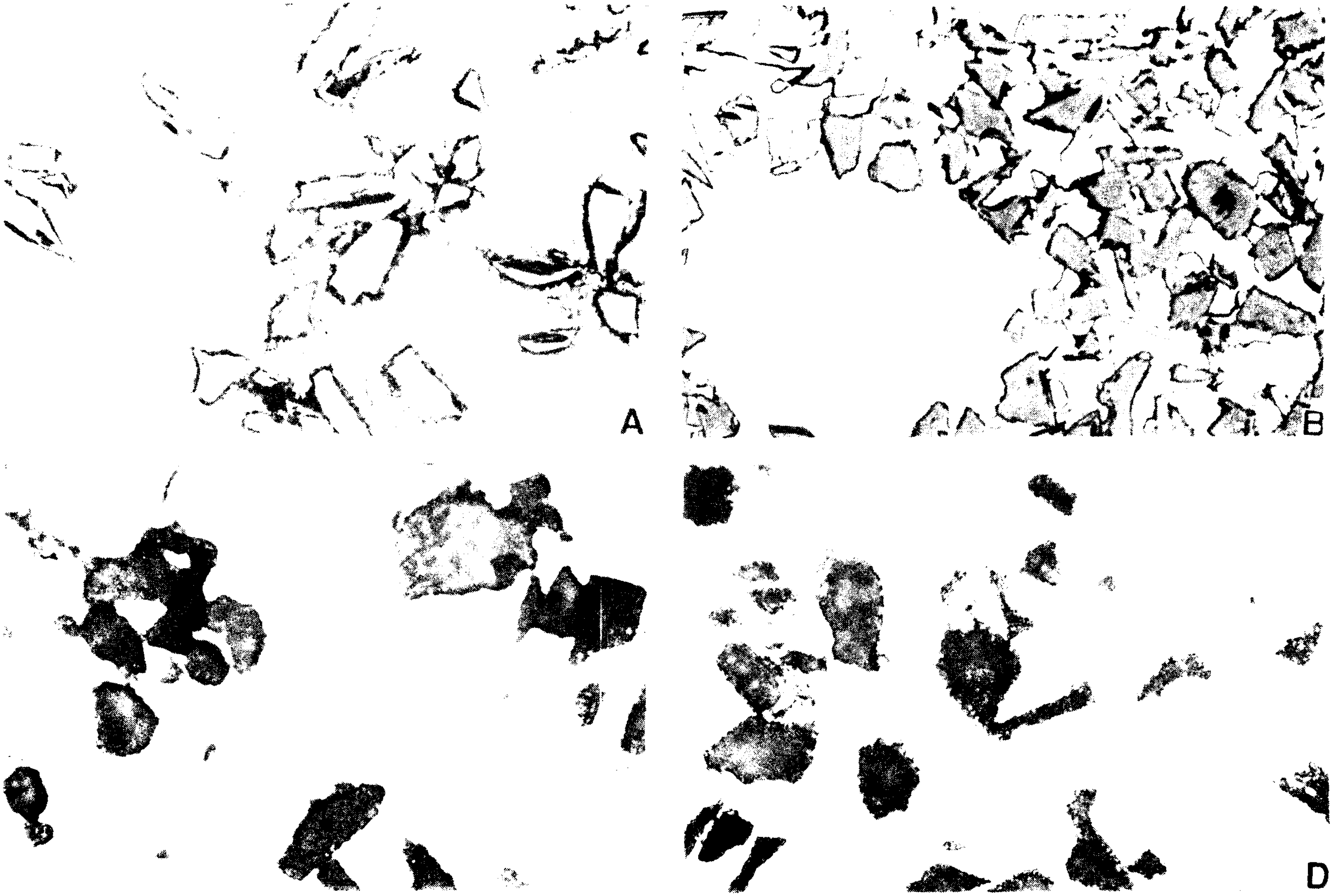

Figure 16. Optical micrographs of MMCs etched with Kellers reagent at 1000x
A) 356+20% SiC sq cast; B) 356+15% SiC billet; C) 6061+15% Al_2O_3 extrusion;
D) 6061+15% Al_2O_3 sq cast.

Conclusions

The metal matrix composites processed by squeeze casting techniques were not free from reinforcement segregation and preferential corrosion susceptibilities. They were only marginally superior to extruded and continuous cast materials. All materials, extruded, billet cast and squeeze cast were found to show significant preferential microstructural corrosion wherever they formed clusters. It was largely attributed to formation of a secondary phase or phases which must have different elemental composition than the matrix. Electrochemical controlled potential corrosion and optical microscopic examinations were highly useful in arriving these conclusions. Between the alumina and silicon carbide as reinforcement material, SiC particulates showed a little poorer distribution than alumina during extrusion. However, it was opposite during squeeze casting. Probably, the thermal conductivities were the primary reasons. During squeeze casting heat is contained and confined for a longer period, thus the particulate distribution could occur more homogeneously. With alumina as particulate material, a thinning of the particles is possible as Al_2O_3 can be reduced to Al during processing. This in turn could change the matrix chemistry and create different microstructural compositions. It could be also the reason why Al_2O_3 containing composites could show some preferential corrosion behavior even in the matrix material.

Acknowledgment

The authors gratefully acknowledge the support of Dr. A. John Sedriks, Office of Naval Research and the Office of Science & Technology, Naval Air Development Center. The supply of metal matrix composite materials by Dr. S. K. Verma, I.I.T. Research Institute, Chicago, IL is highly appreciated.

References

1. R.C. Paciej and V.S. Agarwala, "Metallurgical Variables Influencing the Corrosion Susceptibility of a Powder Metallurgy Aluminum/SiCw Composite", Corrosion, Vol.42, 718-729, 1986.

2. D.M. Aylor and P.J. Moran, "Effect of Reinforcement on the Pitting Behavior of Aluminum-Based MMC", DTNSRDC/SME-85/42, David Taylor Naval Ship Research and Development Center, Annapolis, Maryland, July 1985.

3. R.C. Paciej and V.S. Agarwala, "Influence of Processing Variables on the Corrosion Susceptibility of Metal Matrix Composites", Corrosion, Vol.44, p.680-684, 1988.

4. J.E. Schoutens, "Discontinuous Silicon Carbide Reinforced Aluminum Metal Matrix Composites Data Review", MMCIAC Databook Series MMCIAC NO. 000461 p.5-217, Dec. 1984.

5. D.L. McDaniels, "Analysis of Stress-Strain, Fracture and Ductility Behavior of Aluminum Matrix Composites Containing Discontinuous Silicon Carbide Reinforcement", NASA Technical Memorandum 83610, p.7, March 1984.

6. T.G. Nieh, R.F. Korlak, J. Mater. Sci. Let., Vol.2, p.119-122, 1983.

7. A.P. Divecha, S.G. Fishman and S.D. Karmarkar, J. Metals Vol.9, p.12-17, 1981.

8. I.A. Ibrahim, F.A. Mahomed and E.J. Lavernia, "Particulate Reinforced Metal Matrix Composites-Review", J. Mater. Sci., Vol.26, p.1137-1156, March 1991.

9. S.P. Ray and O.I. Yum, " Squeeze-Cast Al2O3/Al Ceramic-Metal Composites", AM. Ceram. Soc. Bull., Vol.70(2), p.195-197, Feb 1991.

10. Metals Corrosion, Erosion, and Wear, "Laboratory Immersion Corrosion Testing of Metals", 1985 Annual Book of ASTM Standards, Vol 03.02, Philadelphia, PA 19103.

11. Metals Corrosion, Erosion, and Wear, "Conventional Applicable to Electrochemical Measurements in Corrosion Testing", 1985 Annual Book of ASTM Standards, Vol 03.02, Philadeiphia, PA 19103.

12. Metals Corrosion, Erosion, and Wear, "Standard Reference Method for Making Potentiostatic and Potentiodynamic Polarization Measurements", 1985 Annual Book of ASTM Standards, Vol 03.02, Philadelphia, PA 19103.

13. D.O. Kennedy, "SiC Particles Beef Up Investment-Cast Aluminum", Adv. Mater. & Proc., p.42-46, 1991.

14. P.P. Trzaskoma, "Pit Morphology of Aluminum Alloy and Silicon Carbide/Aluminum Alloy Metal Matrix Composites", Corrosion, Vol.46, p.402-409, 1990.

Chief, Materials & Processes
Boeing Aerospace
P.O.Box 3707
Seattle, WA 98124

Chief, Materials & Processes
Lockheed Aircraft Corporation
2555 North Hollywood Way
Burbank, CA 91503

Chief, Materials & Processes
McDonald Douglas Corporation
P.O.Box 516
Saint Louis, MO 63166

Cleveland Pneumatic Corporation
3781 East 77th Street
Cleveland, OH 44105

Chief, Materials & Processes
Vought Corporation
P.O.Box 5907
Dallas, TX 75222

Chief, Materials & Processes
Rockwell International
4300 East Fifth Street
Columbus, OH 43216

Dr. B. Rath
Code 630
Naval Research Laboratory
Washington, DC 20375

Dr. Edward McCafferty
Code 6314
Naval Research Laboratory
Washington, DC 20390

Dr. R. Sutula
Code R33
Naval Surface Warfare Center
Silver Springs, MD 20910

Head, Materials Division
R & D Department
Naval Surface Weapons Center
Silver Springs, MD 20910

Dr. John Gudas
Code 2810
David Taylor Research Center
Annapolis, MD 21402

Mr. I. Kaplan
Code 0115
David Taylor Research Center
Annapolis, MD 21402-5067

Dr. R.G. Kasper
Code 4493
Engineering Mechanics Division
Naval Underwater Systems Center
New London, CT 06320

Mr. J. Hall
Code G53, Materials Group
Naval Surface Warfare Center
Dahlgren, VA 22448

Mr. A.J. D'Orazio
Code PE-72
Naval Air Propulsion Center
Trenton. NJ 08628

Dr. Jeff Perkins
Code 69
Naval Post Graduate school
Monterey, CA 93943

Dr. Joseph Pickens
Martin Marietta Laboratory
1450 South Rolling Road
Baltimore, MD 21227

Dr. Howard W. Pickering
Penn State University
209 Steible Building
University Park, PA 16802

Dr. L. Raymond
L. Raymond Associates
P.O. Box 7925
Newport Beach, CA 92658-7925

Mr. Jules F Senske
ARDC Bldg.355
Dover, NJ 07801

Mr. Paul Shaw
Grumman Aircraft Systems
Bethpage, NY 11714-3582

Dr. Glenn E. Stoner
Dept. of Materials Science &
Engineering
University of Virginia
Charlottesville, VA 22901

Dr. Barry C. Syrett
Electric Power Research Institute
3412 Highview Avenue
P.O.Box 10412
Polo Alto, CA 94303

Dr. H. Townsend
Homer Research Laboratories
Bethlehem Steel Corporation
Bethlehem, PA 18016

Dr. S.K. Varma
IIT Research Institute
10 West 35th Street
Chicago, IL 60616

Dr. Bryan E. Wilde
Fontana Corrosion Center
The Ohio State University
Columbus, OH 43210

Chief, Materials & Processes
Grumman Aerospace
Bethpage, LI, NY 11714

Commanding Officer
Naval Aviation Depot
Jacksonville, FL 32212

Commanding Officer
Naval Aviation Depot
Norfolk, VA 23511

Commanding Officer
Naval Aviation Depot
North Island
San Diego, CA 92135

Commanding Officer
Naval Aviation Depot
Pensacola, FL 32508

Commanding Officer
Naval Aviation Depot
Marine Corp. Air Station
Cherry Point, NC 28533

Commander
Naval Air Force
U.S. Atlantic Fleet
Code 5281
Norfolk, VA 23511

Commander
Naval Air Force
U.S. Pacific Fleet
Attn: Code 7412
San Diego, CA 92135

Commander
Naval Sea Systems Command
Washington, DC 20362

Naval Weapons Center
Attn: Dr. R. Derr
Code 38
China Lake, CA 93555

Dr. James J. Carney
Naval Air Propulsion Center
PE-31 P.O. Box 7176
Trenton, NJ 08628

Mr. Anthony Corvelli
Code 36621
Naval Underwater Systems Center
Newport, RI 02841

Electrochemical Technology Corp.
3935 Leary Way N.W.
Seattle, WA 98109

Dr. D.J. Duquette
Rensselaer Polytechnic Institute
Materials Engineering Department
Troy, NY 12181

Dr. John Green
Martin Marietta Laboratories
1450 South Rolling Road
Baltimore, MD 21227

Dr. Norbert D. Greene (U-136)
University of Connecticut
Storrs, CT 06268

Dr. M.W. Kendig
Rockwell International Science
Center
1049 Camino Dos Rios, P.O.Box 1085
Thousand Oaks, CA 91360

Dr. J. Kruger
Dept. of Materials Science &
Engineering
Johns Hopkins University
Baltimore, MD 21218

DR. M.R. Louthan
Materials Engineering Dept.
Virginia Polytechnic Institute
Blacksburg, VA 24061

Dr. Florian Mansfeld
VHE714
Dept. of Materials Science
University of Southern California
Los Angeles, CA 90009-0241

Dr. C. McMahon, LRSM
University of Pennsylvania
Philadelphia, PA 19104

Dr. Joe H. Payer
Dept. of Metallurgy & Materials
Science
Case Western Reserve University
10900 Euclid Avenue
Cleveland, OH 44106

DISTRIBUTION LIST

Commander
Naval Engineering Facilities Command
Attn: Mr. J. Kaminsky, Code 183
200 Stovall St.
Alexander, VA 223332

Mr. Joseph Collins (AIR 5304)
Naval Air Systems Command
Washington,DC 20361

Dr. L. E. Sloter (AIR 931A)
Naval Air Systems Command
Washington, DC 20361

Dr. John Sedriks
Code 1131
Office of Naval Research
800 North Quincy Street
Arlington, VA 22217

Dr. Richard W. Drisco
Code 152
Naval Civil Engineering Laboratory
Port Hueneme, CA 93043

Ms. Jennie L. Koff
Code L 74
Naval Civil Engineering Laboratory
Port Hueneme, CA 93043

Mr. J.J. Kelly
Office of Naval Technology
800 North Quincy Street
Arlington, VA 22217

Dr. A.K. Vasudevan
Code 1216
Office of Naval Research
800 North Quincy Street
Arlington, VA 22217-5000

Mr. M. Kinna
Office of Naval Technology
800 North Quincy Street
Arlington, VA 22217

Commanding Officer
Naval Aviation Depot
Alameda, CA 94501

Dr. Alan Rosenstein
U.S.Air Force
Office of Scientific Research
Bolling AFB, Washington, DC 20332

Mr. R. Kinsey
MMEMC
Air Force Logistics Center
Warner-Robins AFB
Warner, GA 31908

Mr. Milton Levy
SLCMT-M
U.S. Army Materials & Mechanics
Research Center
Watertown, MA 02172-0001

Dr. Robert Reeber
U.S.Army Research Office
P.O.Box 12211
Research Triangle Park, NC 27709

Belvoir Research, Development &
Engineering Center
Mr. Dario A. Emeric (STRBE-VC)
Fort Belvoir, VA 22060-5606

DR. Phillip Parrish
Defense Advanced Research Projects
Agency
1400 Wilson Blvd. (6th Floor)
Arlington, VA 22209

Dr. Charles G. Interrante
Corrosion Group, Metallurgy Div.
National Bureau of Standards
Washington,DC 20234

Dr. E.N. Pugh
Room B254, Bldg.223
National Bureau of Standards
Washington, DC 20234

Defense Technical Information Center
Attn. DTIC-DDA-1
Cameron Station, Bldg. 5
Alexandria, VA 22314

Dr. Theodore R. Beck